Effect of DC biasing in 3-legged 3-phase transformers taking detailed model of off-core path into account

Abbas Lotfi, Hans K. Høidalen, Nicola Chiesa

***Abstract*—modeling of 3-legged, 3-phase transformers under DC biasing is a challenging topic due to the need to have an adequate representation of flux paths beyond the active part including the tank. The main contribution of this paper is to present a new dual circuit model which takes the off—core flux path into consideration. An equivalent circuit is developed for this off-core path including equivalent non-linear branches for the tank elements. The adequacy of the proposed method is verified through zero sequence impedance tests at steady state. Having the new model, the behavior of a test transformer is studied under DC excitation in terms of magnetization current, reactive and active power flowing through the transformer.**

***Keywords*: Transformer Modeling, DC Biasing, Duality Circuit Model, Off-Core Flux Path, FEM, geomagnetically induced currents**

I. Introduction

Modeling of transformers exposed to DC excitation is the subject of several papers published recently [1-5]. DC biasing of transformers is mainly due to geomegnetically induced currents (GIC) events and observed in HVDC converter transformers as well [6-8]. A DC current flowing through the windings generates a DC flux in the core with a magnitude depending on the magnitude of the DC current, number of turns in the windings carrying the current and reluctance of the DC flux path. This impressed DC flux shifts the operating point of the magnetizing characteristic and causes half cycle saturation in the core resulting in harmonic currents, forcing the flux to flow outside the core and increased reactive power consumption [9]. The important aspects to consider for analyzing a DC biased power transformer are the topology of the core, the nonlinearity of ferromagnetic materials, the coupling and connection of coils, and the system series resistances. The models used for analyzing DC biasing situation are categorized in two FEM-based models [10, 11], and magnetic circuit models [11-16]. The FEM models can be very accurate particularly for the cases where power losses and temperature rises in the tank and other metallic components are of interest. However, the requirement of detailed design information and the computational burden makes the application of FEM modeling not viable for power system studies.

The models based on magnetic circuit theory have been widely used for the analysis of GIC effects on transformers. Some models consider only very basic magnetic circuits lacking a topological representation of the core structure and DC flux paths, and using only simple calculation of model parameters [3, 11]. More advanced models proposed for GIC studies are based on a topologically correct core representation modeling independent core sections and air-flux paths [1, 17-18].

DC flux impressed in the windings is in the same direction for all legs, therefore the flux will flow through the zero sequence flux (ZSF) path. In the case of three-phase three-leg constructions, the ZSF goes outside the core, flows through the air gap and tank and returns to the core. For five-leg constructions, the lateral legs act as return paths for ZSF. As long as they do not saturate, the air-paths and the tank will have no considerable effect. For high level of DC excitation the lateral legs saturate and part of the flux flows outside the core through the oil and the tank leading to increased losses and the temperature rise in the tank.

This paper contributes with a modeling approach for the analysis of the effect of DC excitation in power transformers with focus on off-core flux path modeling. A detailed equivalent circuit is presented for the mentioned off-core path including the non-magnetic space beyond the windings and the tank. Applying the model to a 3-legged 3-phase transformers, the impact of DC flux offset is studied in terms of harmonic content of the magnetizing current, average power losses in of the tank wall, cover and bottom, increase of the reactive and active power flowing through the transformer and copper losses in the windings. Section II describes the transformer model used in the simulations and the equivalent circuit proposed for off-core flux path. Section III describes the system topology and the results of simulations. Section IV discusses on the calculations and differences on alternatives considered for the off-core path.

This work was supported in part by the KMB project " Electromagnetic transients in future power systems" at SINTEF energy research financed by the Research Council of Norway and by Dong Energy, EdF, EirGrid, Hafslund, National Grid, Nexans, RTE, Siemens WP, Statnett, Statkraft, and Vestas WS.

A. Lotfi and H. Kr. Høidalen are with Norwegian University of Science and Technology (NTNU), Electric Power Engineering Department, N-7034 Trondheim, Norway, (abbas.lotfi@ntnu.no).
N. Chiesa is with Statoil AS, Trondheim, Norway, (nchie@statoil.com)

Paper submitted to the International Conference on Power Systems Transients (IPST2015) in Cavtat, Croatia June 15-18, 2015.

II. The Proposed Model

Fig. 1 shows overall dual circuit model of 3-legged 3-phase transformer considered for analyzing DC biasing condition. The difference between this equivalent circuit and conventional dual circuit models [19-21] is the use of detailed equivalent circuit for off-core flux path as shown within blue dashed circle for phase A. There is the same for other two phases. Since the tank elements encompasses all three phases, there should be a magnetic coupling between the phases through these elements. This fact is modeled by means of ideal transformers with unit turns ratio connecting the tank elements to each winding as shown in Fig. 1 where the circuit corresponding to the cover and bottom is not shown in order to make the figure more readable. Fig. 2 illustrates how the mentioned off-core equivalent circuit is obtained from the magnetic structure. As can be seen, the linear inductances (L_1..L_5) represent non-magnetic space beyond the windings (oil gaps) and non-linear branches represent the tank elements.

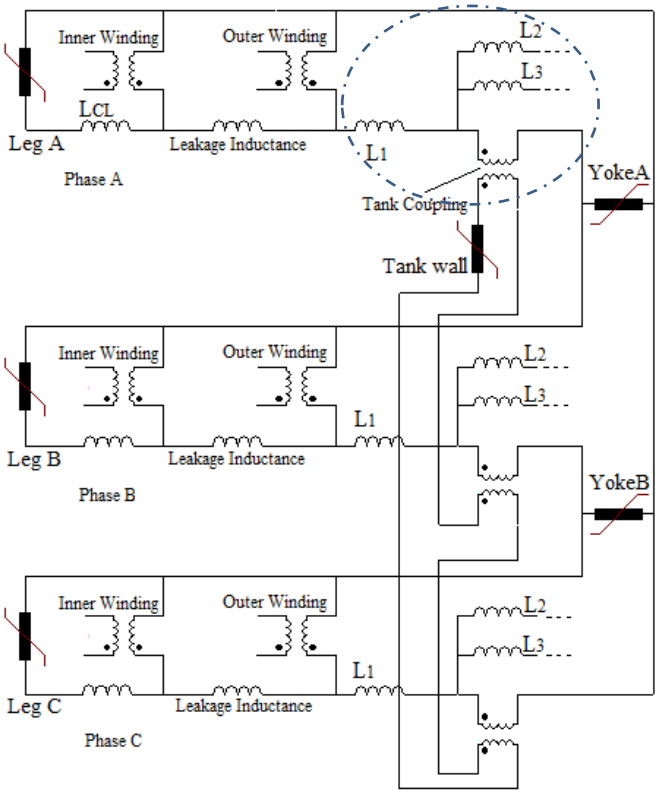

Fig. 1: Transformer equivalent circuit

In order to calculate the linear inductances of L_1...L_5, 3D-FEM models of transformers under study are made in commercial FEM solver of ANSYS-Maxwell (v.16) using the static formulation. In the FEM simulations the tank elements (The wall, cover and bottom) are not taken into calculation and the equivalent impedance of each is set to extreme values of zero or infinite. Zero and infinite values can be achieved by applying flux tangential (T) and flux normal (N) boundary conditions to the each element, respectively. As an example, if flux tangential boundary condition is set to the inner surface of the wall, cover and bottom, the equivalent impedance of corresponding branches will be zero. Then according to Fig.1c, the equivalent off-core inductance seen from the excited winding will be equal to L_1. Accordingly, 5 simulation cases can be defined based on different combination of the boundary conditions set to the tank elements as shown in Table 1 where L_{eqi} is the equivalent off-core inductance seen from the excited winding for the i^{th} simulation case. As can be seen in Table 1, each simulation case leads to an equation with respect to the circuit parameters (L_1…L_5) and the L_{eqi}. The L_{eqi} is obtained by FEM in each simulation case. Then, solving the set of equations (Table I), the parameters will be calculated.

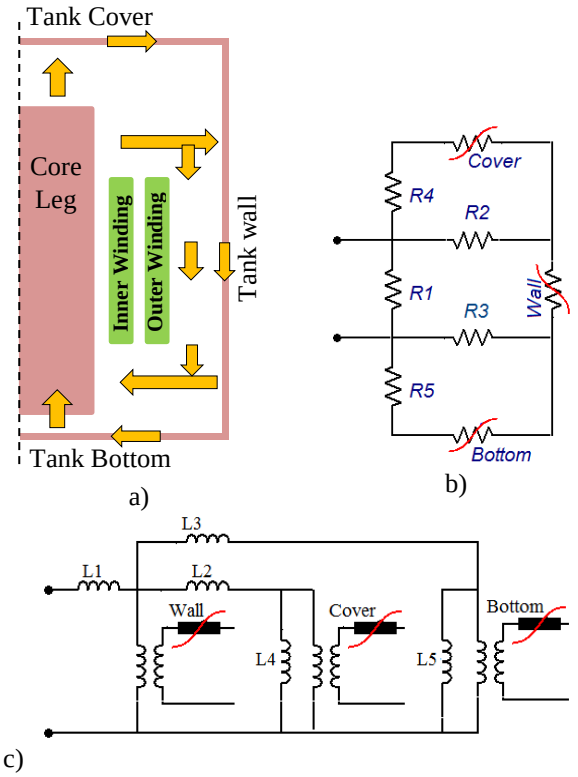

Fig. 2: a) off-core physical flux path b) magnetic circuit c) electric equivalent circuit obtained using duality

TABLE I
SUMMARY OF THE SIMULATION CASE

	Boundary condition			
	Wall	Cover	Bottom	
Case 1	N	T	N	$L_{eq1} = L_1 + (L_3 + L_5)\|\|(L_2 + L_4)$
Case 2	T	T	T	$L_{eq2} = L_1$
Case 3	N	T	T	$L_{eq3} = L_1 + L_2\|\|L_3$
Case 4	N	T	N	$L_{eq4} = L_1 + (L_3 + L_5)\|\|L_2$
Case 5	N	N	T	$L_{eq5} = L_1 + (L_2 + L_4)\|\|L_3$

In order to represent the tank elements two equivalent circuit are used. The first one is a parallel equivalent circuit (PEC) as shown in Fig. 3. Non-linear inductance L_{DC} represents DC magnetization characteristic of the tank elements and non-linear resistance R_e represents classical eddy current loss. The main idea behind this equivalent

circuit is the principle of loss separation where losses due to the magnetic field are divided in two parts including hysteresis and eddy current losses. In a general case non-linear inductance can be replaced with a static hysteresis model. Ignoring hysteresis losses and utilizing DC normal curve, the characteristics of L_{DC} and R_e can be obtained by (1) and (2).

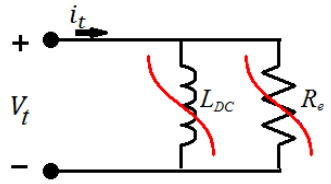

Fig. 3 Parallel equivalent circuit of the tank elements

The characteristics of L_{DC} and R_e are obtained using (1) and (2).

$$\lambda_{DC} = N \cdot t_d \cdot l_t \cdot f_{BH}(\frac{N}{h_e} i_t) \tag{1}$$

$$V_r = N \int R'_e \, di'_t \tag{2}$$

whereas:

$$R'_e = (\frac{l_t}{h_e})(\frac{1}{\sigma \cdot \delta_m})F_{zr} \tag{3}$$

where f_{BH} is a single value DC normal curve, t_d, h_e and l_t are the thickness, the effective height and length of the tank elements, respectively, σ is the electric conductivity of the tank material, N is the turn number of exciting winding, δ_m is the effective magnetic penetration depth stated more in the following. F_{zr} is obtained by (16) and to ensure that the penetration depth is limited to the tank thickness [19].

$$F_{zr} = \frac{\sinh(\zeta)+\sin(\zeta)}{\cosh(\zeta)-\cos(\zeta)} \tag{4}$$

where $\zeta = \frac{2t_d}{\delta_m}$.

The current i'_t and i_t are related to the magnetic field H by $i'_t = H \cdot h_e$ and $i_t = \frac{i'_t}{N}$.

The penetration depth of the magnetic fields δ_m can be obtained by solving the magnetic diffusion equation in a magnetic medium whose B-H relation is given. Assuming that the tank behaves as a linear material at weak excitations, the effective penetration depth is defined in the same way as classical relation of $\sqrt{2/\omega\sigma\mu_m}$ where μ_m is the surface equivalent permeability obtained by the surface field values ($\mu_m = \frac{B_s}{H_s}$). In order to take the impact of saturation, 1D magnetic diffusion equation is solved in a half-space considering a simple saturation curve of $B = kH^{\frac{1}{n}}$ $(n > 1)$ [20]. Equation (5) shows the formula obtained for surface impedance.

$$Z_s^n = (\frac{2n}{n+1})^{\frac{1}{4}} \sqrt{\frac{\omega\mu_m}{\sigma}} e^{j tan^{-1}(\sqrt{\frac{n+1}{2n}})} \tag{5}$$

For the values $n > 7$ and doing some manipulation, the real part of Z_s^n becomes $1/(\sigma \frac{1}{1.4}\sqrt{2/\omega\sigma\mu_m})$ illustrating the effect of saturation as a reduction in the penetration depth.

It must be noted that the approach stated above applies only for steady state simulations. However, is sufficient for DC biasing simulation of transformers due to very slow behavior of GIC events.

The second model of the tank elements being called transient model is obtained by finite difference (FD) approximation of one dimensional form of magnetic diffusion equation in the tank elements as shown in Fig. 4. In this approach the thickness of the tank is subdivided into smaller sections assuming uniform distribution of magnetic flux in each. Fig. 4 shows this detailed FD model. The resistors represent eddy current path and the non-linear inductors represent the path of magnetic flux which are obtained by (6) and (7), respectively.

$$R = \frac{n \cdot l_t}{\sigma t_d \cdot h_e} \tag{6}$$

$$\lambda_i = N \cdot h \cdot l_t \cdot f_{BH}(\frac{N}{h_e} i_i) \tag{7}$$

where n is the number of sub-divisions.

L_{air} represents the air space beyond the tank wall and can be estimated by $\frac{\mu_0 t_d l_t}{h_e}$.

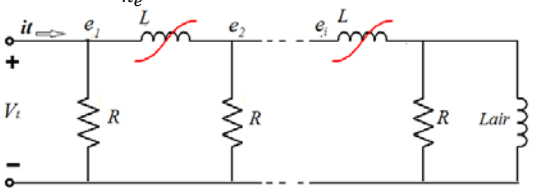

Fig. 4 Detailed FD equivalent circuit for each of tank elements

In order to verify the off-core model and studying the DC biasing situation, a 3-phase 3-legged transformer of 300 kVA is studied under different levels of DC biasing. This unit has two Y-connected windings with voltage level of 11.430 kV/0.235 kV. Design information including the winding and core dimensions, the tank dimension and its distances to the active part as well as a complete test results including open circuit zero sequence tests in a wide range of excitation is available [21]. The linear inductances of $L_1 \ldots L_5$ are calculated making 3D-FEM model of the unit. Since the tank is not modeled and the eddy current effect of the core is not taken into account, static formulation of magnetic potential is used. Once the inductance matrix of the windings is calculated in each simulation case (Table I) by means of energy method, off-core equivalent inductances (L_{eqi}) are calculated by the approach stated in Appendix 1. In the FEM simulations, automatic adaptive meshing is used to refine the elements sizes in each pass of running until the energy error becomes less than 0.05%. The calculation results are presented in Appendix 2. Additionally, magnetic measurements are done on the steel utilized in the tank. Fig. 5 shows the DC normal curve and the losses component. As can be seen in Fig. 5b, the eddy current loss is well larger than the hysteresis one ensuring that neglecting the hysteresis loss does not make large violation in accuracy. Since the measured curve is not monotonically increasing and has many fluctuations, it is approximated by (8) using non-linear least square method.

$$B = \lambda \tan^{-1}(m \cdot H^2) + m_{inf} \cdot H \tag{8}$$

where m, λ and m_{inf} are fitting parameters and adjust the curve slope at the weak fields, knee point and final slope at saturation, respectively. The fitted parameters are $\lambda = 1.09$, $m = 3.59 \times 10^{-6}$ $m_{inf} = 1.47 \times 10^{-5}$. Fig. 5a shows the fitted curve that illustrates good fitting capability of (8) to the measured one.

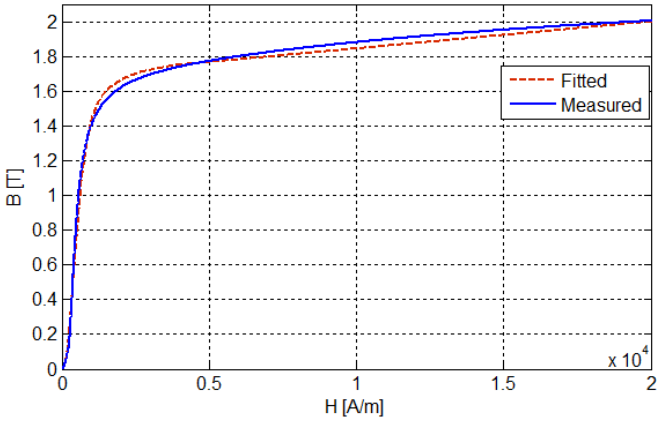

a) Measured DC normal curve of the tank steel

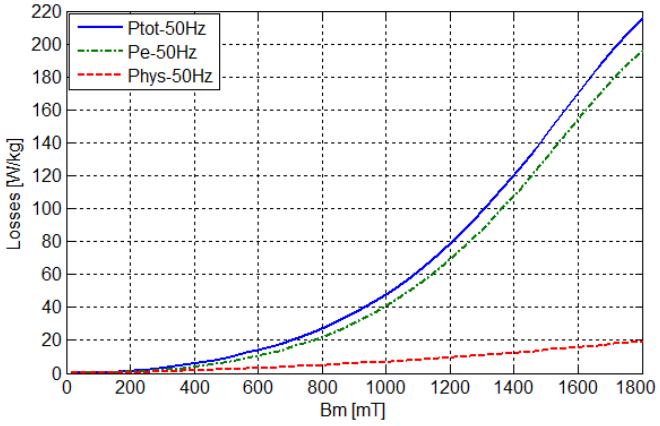

b) Losses measured for the sample of 4 mm thickness

Fig. 5 Magnetic measurements done on the tank steels

Non-linear branches of the main legs and yokes are modeled by a parallel R-L circuit with constant resistance and a non-linear inductance representing core losses and linkage flux-current characteristics of the core, respectively. Parameters of the core are estimated by a fitting approach to the no-load test results as discussed in [22-24]. Leakage inductances and winding resistances at rated frequency are estimated using short circuit test results [23]. Since the magnetizing current gets higher order harmonics with high magnitudes in the case of DC biasing, in order to have an accurate estimation of winding losses foster equivalent circuit with two cells is used to represent the primary winding resistance which has one layer with 21 turns. Equation (9) is used to estimate the resistance at higher frequencies [25].

$$Z(\omega) = R_{DC} \cdot \xi \cdot \coth \xi \qquad (9)$$

where R_{DC} is DC resistance of the winding and $\xi = d\sqrt{j\omega\mu\sigma}$.

III. Simulation System Topologies and the Results

Fig. 6 shows the system topology used for the simulations. Assuming that the transformer is located at the sending end of transmission line, a DC voltage is applied to the neutral point of the secondary windings (HV side), while the primary (LV side) is connected to the network with stiff voltage source. To avoid a step excitation and to resemble the slow nature of GIC, the DC voltage is applied with a ramping time between 3 and 10 s.

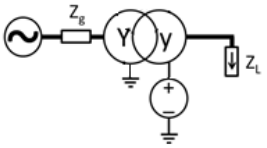

Fig. 6 System topologies used in the simulations

The transformer is loaded at 70% with $Z_L = 10 + j\omega 6.27$. Z_g is a negligible resistive series source impedance of 20 mΩ.

Fig. 7 shows the magnetizing current under DC excitation. As can be seen, the core does not saturate right after applying the DC current. In fact, during the first moments when the DC current is increasing, there is a coupling between primary and secondary side leading to a DC voltage induced on the primary side. During this phase, the leakage inductance and the winding resistances determine the characteristics of the circuit against DC excitation. Increasing the DC current and getting large enough to move the magnetic operating point beyond the knee point of the B-H curve, the core starts to saturate. After reaching the DC current at its final value, equilibrium condition is established. Harmonic content of the magnetizing current is also of interest and is shown in Fig. 8.

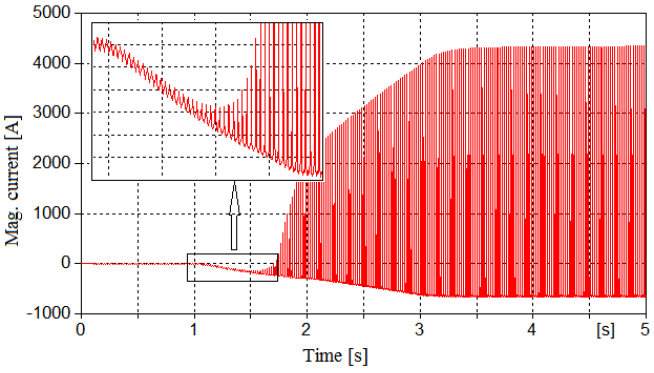

a)

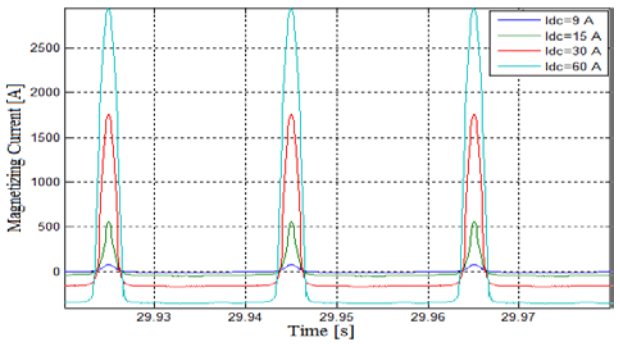

b)

Fig. 7 a) Magnetizing Current for I_{DC}=100 A, b) Equilibrium magnitude

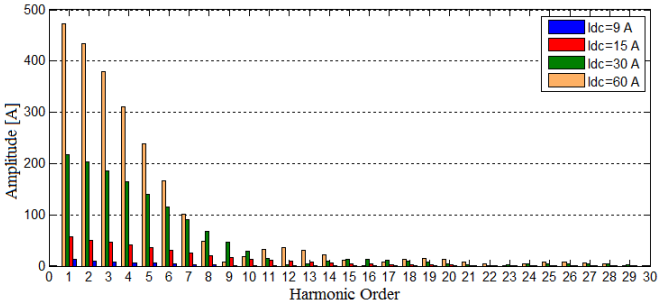

Fig. 8 Harmonic content of magnetizing current

As can be seen in Fig. 8, even order harmonics are increasing dramatically and this can be important in protection system settings [5, 25]. At normal operation, only odd orders of harmonics exist in magnetizing current usually, and up to 7 orders are significant (Fig. 9).

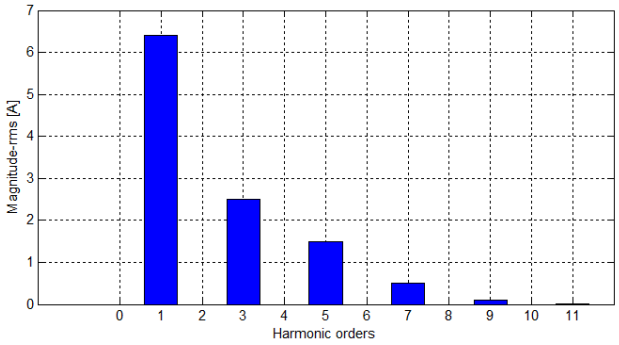

Fig. 9 Harmonic content of magnetizing current at normal operation

In addition to the magnetizing current the losses generated in the tank elements are also important. However, as can be seen in Fig. 11, the power losses in the wall, cover and bottom in presence of a 100 A DC current is not remarkable. The average values of the losses are 1.82, 0.683 and 0.0013 kW for the wall, cover and bottom, respectively.

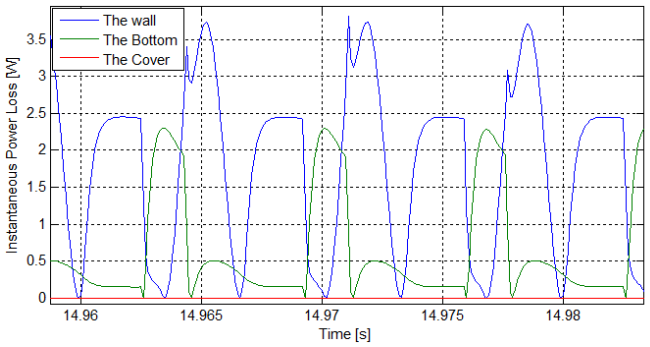

Fig. 11 Instantaneous power losses in the tank elements with I_{dc}=100A.

It should be noted that Fig. 11 gives total power losses in the tank elements and includes no information about hotspots in the wall. In order to study any probable changes in hotspots FEM based modeling must be considered. Moreover, in this case only DC component of the flux leaves the core and flows through the tank wall that does not generate eddy current losses. Fig. 12 shows the flux linkage in the tank elements in the case of I_{dc}= *45* before and after applying DC current.

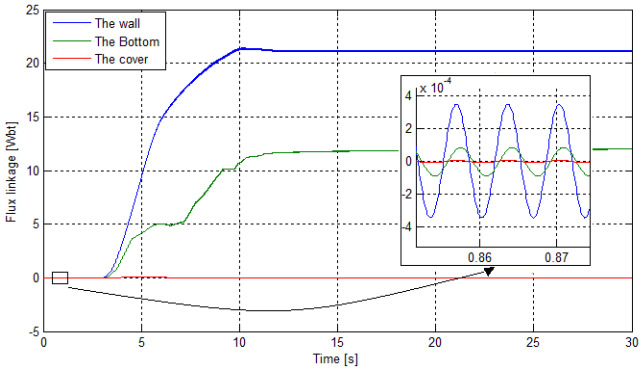

Fig. 12 Flux linkage in the tank elements at I_{dc}=45 A.

The main purpose of using the off-core circuit is to predict the reactive and active power variations as well as magnetizing current of the transformer rather than predicting the hotspots of the metallic components within the tank. As will be shown in the next section, the use of linear inductances instead of detailed circuit of the flux path beyond the windings can make larger errors in higher levels of DC excitation.

Fig. 13 and Fig. 14 show reactive and active power drawn from the primary side. As can be seen, there is a high increase in active and reactive powers due to DC biasing.

It is worth to mention that turn number of HV coil is rather large (1022 turns) making the DC biasing very effective even in 3-legged design where there is high reluctance air path against DC flux. Linearly change of the powers versus of DC current is also reported in other papers [2, 3, 26]. A part of the losses is due to the winding resistances known as copper losses. Fig. 15 shows how this is influenced by DC biasing condition.

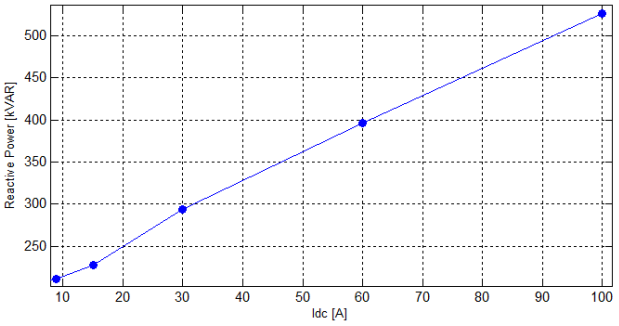

Fig. 13 Reactive Power increasing versus DC current

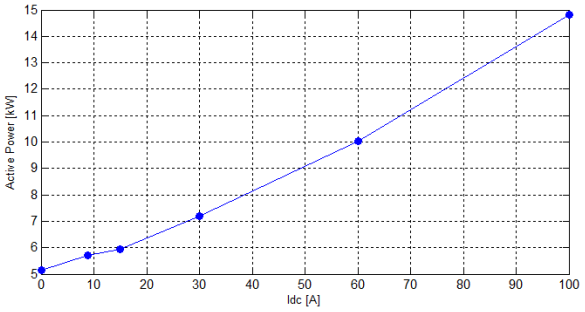

Fig. 14 Active Power increasing versus current

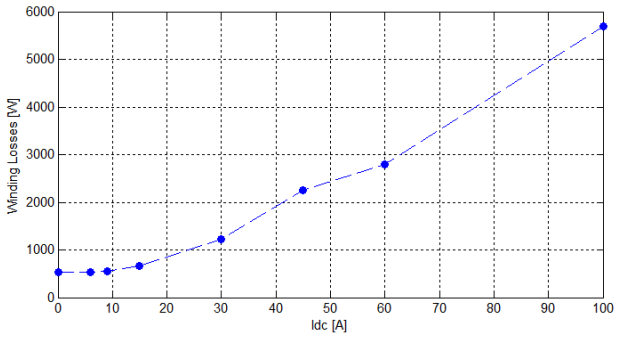

Fig. 15 Copper losses of the transformer

IV. Comparison of Different Off-Core Models

The simplest approach of the off-core path modeling is to use three linear inductances obtained from zero sequence impedance test. It is equal 0.44 mH/phase for the transformer under study. In order to investigate any discrepancies made by this simple approach in comparison with complete modeling of the off-core path, sort of simulations are done considering PEC, model of linear single inductance and detailed model of the wall shown in Fig. 4.

Fig. 16, Fig. 17 and Fig. 18 show effective value (RMS) of the magnetizing current, reactive and active power, respectively. As can be seen there is good agreement between three approaches for the DC current less than 45 A. However, for higher DC current, linear single inductance model overestimate the mentioned quantities. The errors between detailed model and the single inductance model at a I_{DC}=*100 A* are 35%, 28% and 52% for the current, reactive and active power, respectively, while they are 13.5%, 10.5% and 12.3% for PEC. Additionally, it is clearly seen in Figures 16-18 that the proposed parallel equivalent circuit follows the trace obtained by detailed model of the wall whereas the single linear inductance model does not.

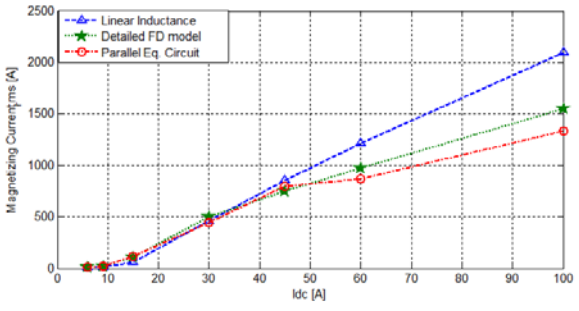

Fig. 16 Magnetizing current obtained by linear, PEC and detailed FD model

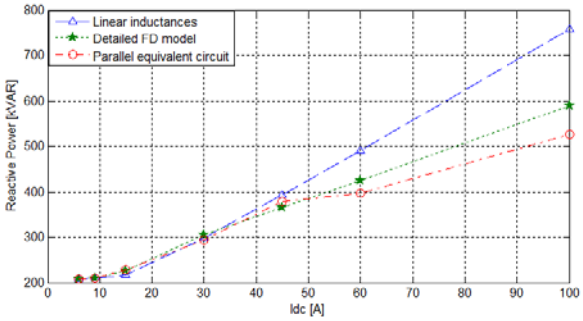

Fig. 17 Reactive power flowing through the transformer

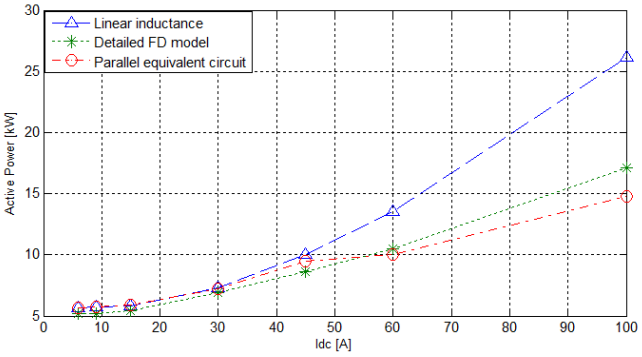

Fig. 18 Active power flowing through the transformer

V. Conclusions

A new approach of the off-core flux path is presented in this paper. This add-on circuit can be used in other types of dual circuit model of transformers. During DC excitation of 3-legged 3-phase transformers the mentioned off-core path play significant role as shown in this paper. A comparison made between three different approach shows that the model of linear single inductance is sufficient at lower excitations. However, at higher DC currents, it starts to deviate from the more accurate model based on FD approximation of the tank wall. While parallel equivalent circuit proposed in this paper shows more accuracy in DC biasing situations and has good agreement with FD based detailed model.

The adequacy of the PEC is also verified by zero sequence impedance test results done on the transformer under study. In order to use the proposed off-core flux path model, it is necessary to have design information including the dimensions of the windings, the core and the tank of transformer and magnetic properties of the material utilized in the tank. As a further work, parameter identification of the model through zero sequence test result can be considered.

VI. References

[1] Hongzhi Li; Xiang Cui; Tiebing Lu; Zhiguang Cheng; Dongsheng Liu,"An improved magnetic circuit model of powertransformers under DC bias excitation", Electromagnetic Compatibility (APEMC), 2010 Asia-Pacific Symposium on, pp. 806 – 809, 2010

[2] Siti, R.M., Hassan, S., Anuar, M.N.K., "Study the harmonic characteristics of DC bias on the single phase power transformer", International Conference on Power Engineering and Optimization (PEDCO) Melaka, Malaysia, 2012, Page(s): 501 – 504.

[3] Jinxia Yao; Min Liu; Changyun Li; Qingmin Li, "Harmonics and Reactive Power of Power Transformers with DC Bias" Power and Energy Engineering Conference (APPEEC), 2010 Asia-Pacific, Pp. 1–4, 2010

[4] W. Zhu. Caihong Yan. Yongjiang Jia, "Research on Large DC-Biased Power Transformer", International Conference on Electrical and Control Engineering (ICECE), 2010, Page(s): 4102 – 4105

[5] W. Zhu. Caihong Yan. Yongjiang Jia, "Research on Large DC-Biased Power Transformer", International Conference on Electrical and Control Engineering (ICECE), 2010, Page(s): 4102 – 4105

[6] R. Pirjola, "Geomagnetically induced currents during magnetic storms," *IEEE Trans. Plasma Sci.*, vol. 28, no. 6, pp. 1867–1873, Dec. 2000.

[7] P. Price, "Geomagnetically induced current effects on transformers," *Power Delivery, IEEE Transactions on*, vol. 17, no. 4, pp. 1002-1008, 2002.

[8] S.Chen, A.R. Wood, J. Arrillaga, "HVDC converter transformer core saturation instability: a frequency domain analysis" Generation,

Transmission and Distribution, IEE Proceedings- , Vol. 143, Issue: 1, 1996, Page(s): 75 - 81
[9] B. Zhang, L. Liu, Y. Liu, M. McVey and R. Gardner, "Effect of geomagnetically induced current on the loss of transformer tank," *Electric Power Applications, IET*, vol. 4, no. 5, pp. 373-379, 2010
[10] Seyed Ali Mousavi, "electromagnetic Modelling of Power Transformers with DC Magnetization", Licentiate Thesis in Electromagnetic Engineering, TRITA-EE 2012:057, ISBN 978-91-7501-537-8, Royal Institute of Technology (KTH), , Stockholm, Sweden 2012
[11] X. Zhao ; J. Lu ; Lin Li ; Z. Cheng ; T. Lu, " Analysis of the DC Bias Phenomenon by the Harmonic Balance Finite-Element Method", IEEE Trans. Power Delivery, Volume: 26 , Issue: 1 , 2011 , Page(s): 475 - 485
[12] Xuzhu Dong; Yilu Liu; Kappenman, J.G., "Comparative Analysis of Exciting Current Harmonics and Reactive Power Consumption from GIC Saturated Transformers", Power Engineering Society Winter Meeting, pp. 318 – 322, vol.1, 2001
[13] Masoum, Mohammad A.S.; Moses, Paul S., "Influence of Geomagnetically Induced Currents on three-phase power transformers", Power Engineering Conference, 2008. AUPEC '08. Australasian Universities, pp. 1–5, 2008
[14] E. F. Fuchs, Y. You, and D. J. Roesler, "Modeling and simulation, and their validation of three-phase transformers with three legs under DC bias," *IEEE Transactions on Power Delivery*, vol. 14, pp. 443-449, 1999.
[15] E. F. Fuchs and Y. Yiming, "Measurement of Lambda-I characteristics of asymmetric three-phase transformers and their applications," *IEEE Transactions on Power Delivery*, vol. 17, pp. 983-990, 2002.
[16] D. Tousignant, L. Bolduc, A. Dutil, "A method for the indication of power transformer saturation", Electric Power Systems Research, Vol. 37, Issue 2, May 1996, 115-120.
[17] Picher, P.; Bolduc, L.; Olivier, G., "Acceptable direct current in three-phase power transformers: comparative analysis", Electrical and Computer Engineering, 1997. Engineering Innovation: Voyage of Discovery. IEEE 1997 Canadian Conference on, pp. 157-160 vol.1, 1997
[18] A. Rezaei-Zare, "Enhanced Transformer Model for Low- and Mid-Frequency Transients—Part I: Model Development ", IEEE Trans. Power Del., Issue 99, 2014
[19] J. Lammeraner, M. Stafl, "Eddy currents", ILIFFE Books LTD, London, 1966.
[20] Isaak D. Mayergoyz, "Nonlinear Diffusion of Electromagnetic Fields: With Applications to Eddy Currents and Superconductivity (Electromagnetism)" Acadenic Press, 1998, ISBN-13: 978-0124808706.
[21] D. Negri, M. Gotti, "Transformer Model Benchmarking", Master thesis, Politecnico di Milano, 2007.
[22] B. A. Mork, F. Gonzalez, D. Ishchenko, D. L. Stuehm, and J. Mitra, "Hybrid transformer model for transient simulation: Part I: development and parameters," IEEE Trans. Power Del., vol. 22, no. 1, pp. 248–255, Jan. 2007.
[23] H. K. Høidalen, B. A. Mork, F. Gonzalez, D. Ishchenko, N. Chiesa: "Implementation and verification of the Hybrid Transformer model in ATPDraw", Electric Power Systems Research 79 (2009), 454-459.
[24] H. K. Høidalen, N. Chiesa, A. Avendaño, B. A. Mork, "Developments in the hybrid transformer model – Core modeling and optimization", IPST, Delft, the Netherlands June 14-17, 2011.
[25] F. de Leon, A. Semlyen, "Time domain modeling of eddy current effects for transformer transients", IEEE Trans. Power Delivery, Vol. 8, No. 1, Jan. 1993.
[26] N. Chiesa, A. Lotfi, H. Hoidalen, et al, "Five-leg transformer model for GIC studies", IPST2013, 2013, Vancouver, Canada.

APPENDIX 1-CALCULATION OF OFF-CORE INDUCTANCES BY MEANS OF INDUCTANCE MATRIX

Once the inductance matrix of the transformers are calculated by 3D-FEM and expressed as $\bar{L} = \begin{bmatrix} [\bar{L}_{HV}]_{3\times3} & [\bar{L}_{HV-LV}]_{3\times3} \\ [\bar{L}_{LV-HV}]_{3\times3} & [\bar{L}_{LV}]_{3\times3} \end{bmatrix}_{6\times6}$, the off-core inductance seen from HV can be calculated by the following equations using only the part $[\bar{L}_{HV}]_{3\times3}$:

$$\bar{V}_{HV} = \bar{L}_{HV} \cdot D\bar{I}_{HV} \rightarrow D\bar{I}_{HV} = \bar{\Gamma}_{HV} \cdot \bar{V}_{HV} \quad \text{(A1-1)}$$

where D is the derivation operator.

If the same voltage is applied to the HV windings (V_0), the flux has no path but outside the core. Then the inductance seen from the terminal is corresponding to the off-core path. The yoke effects are ignored against the oil reluctances.

$$DI_i = \Gamma_{i1}^{HV} \cdot V_0 + \Gamma_{i2}^{HV} \cdot V_0 + \Gamma_{i3}^{HV} \cdot V_0 \rightarrow \Gamma_{off-core,i}^{HV} = \sum_{k=1}^{3} \Gamma_{ik}^{HV}, \; i=1..3, \quad \text{(A1-2)}$$

where $\bar{\Gamma}^{HV}$ is the inverse matrix of $[\bar{L}_{HV}]_{3\times3}$.

On the same way for LV side, using $[\bar{L}_{LV}]_{3\times3}\ \Gamma_{off-core,i}^{LV} = \sum_{k=1}^{3} \Gamma_{ik}^{LV}$.

APPENDIX 2

Table A2-1 Off-core equivalent inductances ($L_{eq,i}$) seen from HV

Simulation cases	*Values[mH]*
Case 1-$L_{eq,1}$	1397.0
Case 2- $L_{eq,2}$	172.7
Case 3- $L_{eq,3}$	1020.8
Case 4- $L_{eq,4}$	1392.7
Case 5- $L_{eq,5}$	1030.0

Table A2-2 Linear inductances in the off-core equivalent circuit seen from HV side

Linear inductances	*Values [mH]*
L1	172.7
L2	2016.3
L3	1463.3
L4	50.0
L5	1594.2